Published in final edited form as:

Biomacromolecules. 2019 February 11; 20(2): 969–978. doi:10.1021/acs.biomac.8b01592.

Coupling Self-Assembly Mechanisms to Fabricate Molecularly and Electrically Responsive Films

Jinyang Li[†,‡], **Drishti Maniar**[†,‡], **Xue Qu**[*,§], **Huan Liu**[§], **Chen-Yu Tsao**[†,‡], **Eunkyoung Kim**[†], **William E. Bentley**[†,‡], **Changsheng Liu**[*,§], **Gregory F. Payne**[*,†]

[†]Institute for Bioscience and Biotechnology Research, University of Maryland, College Park, Maryland 20742, United States

[‡] Fischell Department of Bioengineering, University of Maryland, College Park, Maryland 20742, United States

[§] Key Laboratory for Ultrafine Materials of Ministry of Education, The State Key Laboratory of Bioreactor Engineering, East China University of Science and Technology, Shanghai, 200237, China

Abstract

Biomacromolecules often possess information to self-assemble through low energy competing interactions which can make self-assembly responsive to environmental cues and can also confer dynamic properties. Here, we coupled self-assembling systems to create biofunctional multilayer films that can be cued to disassemble through either molecular or electrical signals. To create functional multilayers, we: (i) electrodeposited the pH-responsive self-assembling aminopolysaccharide chitosan, (ii) allowed the lectin Concanavalin A (ConA) to bind to the chitosan-coated electrode (presumably through electrostatic interactions), (iii) performed layer-by-layer self-assembly by sequential contacting with glycogen and ConA, and (iv) conferred biological (i.e., enzymatic) function by assembling glycoprotein (i.e., enzymes) to the ConA-terminated multilayer. Because the ConA tetramer dissociates at low pH, this multilayer can be triggered to disassemble by acidification. We demonstrate two approaches to induce acidification: (i) glucose oxidase can induce multilayer disassembly in response to molecular cues, and (ii) anodic reactions can induce multilayer disassembly in response to electrical cues.

Graphical Abstract

[*]Corresponding Authors gpayne@umd.edu (G.P.)., liucs@ecust.edu.cn (X.Q.)., quxue@ecust.edu.cn (C.L.).

The authors declare no competing financial interest.

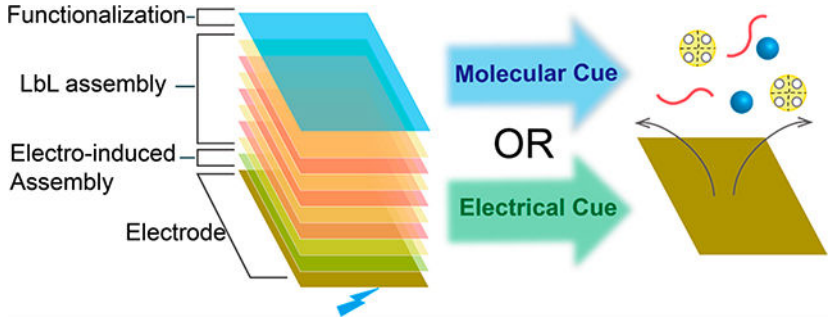

INTRODUCTION

Complex material systems in biology are often held together through a large number of low energy, noncovalent, and, in some cases, biospecific interactions. To create such material systems, in biology, biomacromolecules that possess the intrinsic information needed for bottom-up self-assembly are often enlisted.[1,2] These same biological materials and mechanisms are often enlisted to create hierarchical structures ex vivo[3–5] and to confer useful biological functions to these structures.[6–13] In addition, when material systems are held together by low energy and reversible interaction mechanisms, they often possess dynamic capabilities to heal, respond, and reconfigure.[14–19] Here, we report the coupling of independent self-assembly mechanisms to create a dynamically responsive film that can be cued to disassemble through externally applied molecular or electrical inputs.

Some stimuli-responsive self-assembling biopolymers can be triggered by electrical inputs to deposit on the surface of an electrode, and often such electrodeposition processes are simple, rapid, reagentless, and highly controllable.[20,21] One of the best understood biopolymer electrodeposition processes is the cathodic deposition of the pH-responsive aminopolysaccharide chitosan. At low pH (usually pH < 6), the amine groups of chitosan are protonated making chitosan soluble in aqueous solution.[22] Upon raising the pH, the amine groups become deprotonated, the chitosan chains lose their charge, and can self-assemble into a hydrogel network. These pH-responsive gel-forming properties enable chitosan to be electrodeposited at a cathode surface. Specifically, when a cathodic potential is applied to an electrode that is immersed in acidic chitosan solution, electrolytic reactions yield a high pH region which can trigger the localized self-assembly of chitosan on the electrode surface. Chitosan's electrodeposition confers spatiotemporal selectivity and quantitative control to self-assembly (i.e., chitosan can electrodeposit on a patterned electrode with the electrode-specific dimensions in response to electrode imposed electrical signals).[23,24] Importantly, chitosan-coated electrodes present surface-exposed amine groups that can engage in additional interactions (e.g., electrostatic and/or covalent) for further assembly. As illustrated in Scheme 1a, we use electrodeposition as the first self-assembly step for fabricating multilayer films.

Another convenient aqueous-based method to self-assemble biopolymer films involves layer-by-layer (LbL) methods that can enlist various physical interaction mechanisms and provide a gentle and versatile means to construct multilayer architectures. We fabricate multilayer films using LbL self-assembly and biospecific interactions between the lectin

Concanavalin A (ConA) and the polysaccharide glycogen (a branched polymer of glucose).[25,26] To fabricate this multilayer, ConA is first coated onto the electrodeposited chitosan film through nonspecific and presumably electrostatic binding interactions, then multilayers can be generated by sequentially contacting with solutions of glycogen and ConA. Importantly, ConA contains four sites for binding sugars that include D-glucose and D-mannose, which enables it to serve as a protein-based physical cross-linking agent for the ConA-glycogen multilayers. Also it is important that ConA can bind to glycoproteins with certain glycan structures[27,28] (e.g., enzymes and glycosylated monoclonal antibodies, mAbs), and this enables these self-assembled films to be biofunctionalized.

To create dynamically responsive assemblies, in biology, noncovalent mechanisms that can be reversed by changes in environmental parameters are often enlisted, and one of the most important triggering parameters is pH. For instance, a virus' infection cycle often involves pH-triggered assembly and disassembly of the coat protein,[29–31] while technological efforts to target nanoparticle-based therapeutics often aim to exploit the pH differences associated with the different stages of endosomal uptake.[32,33] Additionally, the binding affinity of glycosylated antibodies can be pH dependent, facilitating their purification and detection.[34] In our case, the assembled ConA-glycogen multilayer is pH-responsive and disassembles at low pH as the ConA tetramer dissociates into dimers[35–37] (note that electrodeposited chitosan will also redissolve at low pH but more slowly). Importantly, various mechanisms exist to transduce alternative cues into the pH changes that can trigger localized disassembly. As illustrated by Scheme 1b, we demonstrate two separate mechanisms to transduce external cues into the pH signals required to trigger ConA-glycogen disassembly: (a) an enzyme that can transduce a molecular signal (i.e., glucose) into H^+ is assembled on the film, allowing film disassembly to be cued by a molecular input, and (b) an electrical signal can be imposed to the underlying electrode to locally generate H^+, allowing film disassembly to be cued by an electrical input.[38–41] Potentially, film disassembly can also be monitored electronically either by detecting changes in structure (e.g., by electrochemical impedance spectroscopy) or function if the function involves the generation of redox-active products (e.g., H_2O_2). Thus, we report the coupling of biological mechanisms to self-assemble a multilayer film capable of molecularly specific enzyme-mediated disassembly or capable of disassembling in response to device-convenient electrical inputs.

MATERIALS AND METHODS

Materials

The following materials were purchased from Sigma-Aldrich: chitosan from crab shells (85% deacetylation), D-(+)-glucose (≥99.5%), glucose oxidase (GOx) from *Aspergillus niger*, Concanavalin A (ConA) from *Canavalia ensiformis*, FITC conjugate (FITC-ConA), 2,2′-azino-bis(3-ethylbenzothiazoline-6-sulfonic acid) (ABTS), and hydrogen peroxide solution. Concanavalin A was purchased from Santa Cruz. Glycogen was purchased from Acros. Horseradish Peroxidase (HRP) was purchased from Shanghai Yuanju Biotech. Gold-coated quartz crystal (QSX338, Au with Ti adhesion layer) was purchased from NanoScience Instrument. The pH indicator (Metacresol Purple Sodium Salt) was purchased from TCI.

Chitosan Electrodeposition—1% chitosan solution was first prepared by slowly dissolving chitosan flakes in diluted HCl after which the pH was adjusted to 5.5 by 1 M NaOH. A gold or platinum electrode was partially immersed into the chitosan solution as the working electrode, with a Pt wire serving as a counter electrode. Chitosan electrodeposition was performed for 5 min at a constant current density of 4 $A \cdot m^{-2}$. The resultant chitosan-coated electrode was rinsed extensively with water and Tris-HCl buffer (100 mM. pH 8.0). To fabricate a free-standing chitosan film, the deposition time was extended to 10 min and the chitosan-coated electrode was exposed to NaOH solution (100 mM) for 30 min after which the chitosan film could be peeled off from the electrode.

LbL Self-Assembly—The chitosan-coated electrode was sequentially contacted with solutions containing ConA and glycogen alternatively each for 30 min (2 mg/mL, in 100 mM Tris-HCl buffer at pH 8.0). After each assembly, three sequential washes by Tris-HCl buffer (each for 5 min) were preformed to remove loosely bound molecules. After several repeated adsorption steps, the multilayer film was obtained and denoted as Chit-(ConA/Gly)$_n$ConA, where n represents the number of multilayers. For the fluorescence study, FITC-labeled ConA was used. To biofunctionalize film with enzymes, Chit-(ConA/Gly)$_n$ConA coated electrode was incubated with solution containing GOx or HRP (5 mg/mL, in 100 mM Tris-HCl buffer at pH 8.0) for 1 h, followed by rinsing with Tris-HCl buffer.

EQCM Monitoring of Assembly—The electrodeposition and LbL self-assembly processes were monitored by EQCM-D (Q-Sense E4, Sweden). A typical three-electrode setup was employed with a gold-coated quartz crystal as a sensor and the working electrode, an Ag/AgCl electrode as the reference electrode, and a Pt wire as the counter electrode. The measurement was conducted at 25 °C. To ensure relatively rigid and thin adhered film fabrication, a 10-fold diluted chitosan solution (0.1%, pH 5.5) was used, and a cathodic voltage of −1.2 V was applied for 1 min, followed by alternate assembly of ConA, glycogen, and GOx layers. Buffer rinsing was performed for 5−10 min after each assembly step.

Electrochemical Impedance Measurement—The impedance measurements were performed by a CHI6273c electrochemical analyzer (CH Instruments) and a typical three-electrode system, where the film-coated or bare standard gold electrode was used as the working electrode, an Ag/AgCl electrode was the reference electrode, and a Pt wire was the counter electrode. The measurements after the formation of each layer were performed in phosphate buffered solution (100 mM, pH 7.4) containing 0.5 mM $K_3Fe(CN)_6/K_4Fe(CN)_6$ over a frequency range of 100 kHz to 1 Hz with an amplitude of 5 mV at the potential of +0.2 V vs Ag/AgCl. The data are represented in the complex plane; Nyquist plots (Z'' vs Z', Z'' = imaginary impedance and Z' = real impedance).

Electrochemical Detection of GOx and Monitoring of Disassembly—The function of GOx was examined electrochemically by the electrochemical oxidation of H_2O_2 generated in a GOx-catalyzed reaction. The electrochemical measurements were performed by current−time (i−t) measurements using a CHI6273c electrochemical analyzer (CH Instruments) and a typical three-electrode system, where the film-coated electrode was used

as the working electrode, an Ag/AgCl electrode was the reference electrode, and a Pt wire was the counter electrode. Initially, the three electrodes were immersed in 5 mL of phosphate buffer (10 mM, pH 7.4, containing 100 mM Na_2SO_4 to ensure electrical conductivity) under gentle stirring while the electrode was biased to +0.7 V and the current output was monitored. Aliquots (10 μL) of a concentrated glucose solution (500 mg/mL) were intermittently added to the solution to increase the glucose concentration by 1 mM.

To monitor disassembly of the GOx-functionalized film in response to high levels of glucose, 50 μL of 500 mg/mL glucose was added and the stirring was suspended to allow accumulation of H^+ on the electrode. After 90 min, the electrodes were rinsed, added to a fresh buffer solution, biased to +0.7 V, and exposed to glucose again in order to detect a loss of GOx function and demonstrate disassembly.

To induce and monitor disassembly of film cued by electrical signal, the electrode was biased to +1.5 V for 10 min without stirring. Subsequently, the electrodes were rinsed, added to a fresh buffer solution, biased to +0.7 V, and exposed to glucose again to demonstrate disassembly.

Characterization of Dual-Enzyme Activity—For film functionalized by both GOx and horseradish peroxidase (HRP), the dual-enzyme activity was characterized by the GOx-catalyzed oxidation of glucose with the generation of H_2O_2 that serves as the cosubstrate for the subsequent HRP-catalyzed conversion of reduced ABTS ($ABTS^{Red}$) into the dark green oxidation product $ABTS^{Ox}$. Experimentally, the film-coated electrode or the free-standing multilayer film was incubated in solution containing H_2O_2 (0.01%) and $ABTS^{Red}$ (5 mM) for 4 h followed by imaging.

RESULTS

Physical Evidence for Film Assembly

Figure 1a shows the films were prepared by (i) electrodepositing the chitosan through a cathodic neutralization mechanism,[24,42] (ii) contacting the chitosan-coated electrode with a buffered solution (pH 8.0) containing ConA (pI 4.5−5.5) to allow this protein to bind through nonspecific (presumably electrostatic) interactions,[22,43,44]and (iii) sequentially contacting the film with glycogen and ConA solutions to enable biospecific layer-by-layer (LbL) self-assembly.[45–48] This assembled film is denoted as Chit-(ConA/Gly)$_n$ConA, where n represents the number of ConA and glycogen bilayers. In initial studies, we biofunctionalized the films using the glycoprotein glucose oxidase (GOx) which assembles through the same biospecific ConA−sugar interactions,[49–54] and this film is denoted as Chit-(ConA/Gly)$_n$ConA/GOx.

In initial studies, FITC-labeled ConA (FITC-ConA) was employed to visualize assembly and demonstrate that films could be assembled onto a patterned electrode with spatial selectivity. Specifically, the initial electrodeposition step confers spatial selectivity as this deposited chitosan film serves as a “template” for subsequent binding of the ConA protein[55] and further LbL self-assembly steps. The images in Figure 1b show that fluorescence was only observed on the electrode addresses and the fluorescence intensity progressively

increased with each additional assembled bilayer. We have previously demonstrated that chitosan electroassembly can be spatially selective;[24] this image indicates that the electrodeposited chitosan film serves as a "template" to confer spatial selectivity to the subsequent ConA-glycogen LbL self-assembly. These results provide initial visual evidence that LbL self-assembly can be coupled with electrodeposition for spatially controllable self-assembly.

Physical evidence for the self-assembly and functionalization of our films is provided by in situ electrochemical quartz crystal microbalance (EQCM) measurements. This technique allows the simultaneous application of an electrical stimulus and the monitoring of film formation on the surface of a gold electrode. In this experiment, the gold-coated QCM crystal was immersed in a chitosan solution (0.1%, pH 5.5) and a cathodic voltage (1.2 V, 60 s) was applied. As shown by the inset in Figure 1b, a rapid decrease in frequency was observed upon the application of voltage, indicating electrodeposition of chitosan. After this brief electrodeposition step, the chitosan-coated crystal was thoroughly rinsed with Tris-HCl (pH 8.0) buffer and then sequentially contacted with ConA, glycogen, and glucose oxidase (GOx). With each contacting step, a decrease in frequency was observed which is consistent with the sequential assembly of each layer.[37] The multiple curves in Figure 1b are data collected at different overtones (n = 3, 5, 7), and the spreading of frequency shift at different overtones indicates that the formed multilayers are rather soft.[56] Because of the significant viscoelastic nature of the assembled films, it may not be accurate to quantify the mass of each layer using the Sauerbrey equation.[56] Nevertheless, the EQCM results demonstrate qualitatively the stepwise LbL self-assembly of multilayers onto electrodeposited chitosan.

Additional physical evidence for the sequential self-assembly and functionalization of our films is provided by electrochemical impedance spectroscopy (EIS) using $Fe(CN)_6^{3-/4-}$ as a redox-specific probe. In this experiment, the electrode surface was contacted with a solution containing $Fe(CN)_6^{3-/4-}$ and probed by imposing small oscillating voltages, measuring the response currents, and determining the impedance. The frequency dependence of this impedance reveals the electrical behavior of the electrode interface due to diffusion, double-layer charging, resistance of the solution (R_S), and charge transfer (R_{ct}).[57–59] Especially, the faradaic impedance spectroscopy techniques using the redox probe ($Fe(CN)_6^{3-/4-}$) can sensitively monitor the change of charge transfer resistance (R_{ct}) dependent on the surface charge developed by the layer-by-layer formation. Figure 1d shows the Nyquist plots of a standard gold electrode after different number of layers had been assembled. The Nyquist plots of the bare electrode and electrode with electrodeposited chitosan were found to be nearly linear, indicating that the transfer of charges was unhindered.[60] After the ConA layer had been assembled on the electrode, the Nyquist analysis shows a semicircular shape at low frequency which indicates that this added ConA layer hinders the diffusion of $Fe(CN)_6^{3-/4-}$ to the electrode surface.[57,61–63] With each subsequent assembly step, Figure 1d shows that the semicircle diameter of the Nyquist plot increases indicating increasing charge transfer resistance (R_{ct}).[57,62–64] Thus, these impedance measurements further demonstrate the coupling of electrodeposition and LbL for multilayer film assembly.

Assembling Biological Function to Multilayer Film

In our initial studies, we conferred biological function to our assembled film by allowing the biospecific binding of GOx to ConA, and we demonstrate this biofunction using electrochemical analysis. As illustrated in Figure 2a, we started with a standard gold electrode and assembled a chitosan and ConA/Gly multilayer with ConA as the outermost layer (Chit-(ConA/Gly)$_3$ConA). We then incubated this film-coated electrode with a GOx solution (5 mg/mL) for 1 h. After thoroughly rinsing the functionalized film, the activity of GOx was measured electrochemically as illustrated by the reactions in Figure 2b. Specifically, the GOx-catalyzed oxidation of glucose generates a redox-active product (H_2O_2) that can be detected electrochemically. Experimentally, we used a three-electrode system with the GOx-functionalized electrode serving as the working electrode. To evaluate the GOx-function, we applied a constant anodic potential (+ 0.7 V) and then sequentially introduced aliquots of a concentrated glucose solution (500 mM) to achieve the stepwise increases in the solution's glucose concentration. As shown by Figure 2c, the output oxidation current showed a rapid increase upon the addition of each glucose aliquot, while the standard curve shows good linearity between output current and glucose concentration (inset plot in Figure 2c). As a control, we assembled a multilayer that lacked GOx on an electrode and observed no appreciable change in output current in response to the addition of glucose. The results in Figure 2 indicate that the assembled GOx confers enzymatic function to the film assembly.

Next, Figure 3a shows the assembly of films biofunctionalized by the sequential biospecific assembly of two glycosylated enzymes: GOx and horseradish peroxidase (HRP).[65–68] Like GOx, HRP is a glycosylated protein that can be assembled onto the film by binding to the sugar-binding sites on ConA. The functions of GOx and HRP were examined by the classic cascade reactions shown in Figure 3b.[69–71] In this reaction cascade, GOx catalyzes the oxidation of glucose to produce H_2O_2, which is then used by HRP to oxidize 2,2′-azino-bis(3-ethylbenzothiazoline-6-sulfonic acid) ($ABTS^{Red}$, colorless) into $ABTS^{Ox}$ (green). Experimentally, we first electrodeposited a chitosan film, peeled it from the electrode,[72,73] and sequentially contacted this film with solutions of ConA, glycogen, and finally, GOx and HRP (5 mg/mL). (Note that the sequence used to assemble GOx and HRP did not affect the results.) After thoroughly rinsing the film, it was incubated (4 h) in a solution containing glucose (5 mM) and $ABTS^{Red}$ (5 mM). The leftmost image in Figure 3c shows that the film assembled with both GOx and HRP was observed to be dark green, presumably because $ABTS^{Ox}$ diffuses into and is bound to the multilayer film. The middle image in Figure 3c shows results for a control Chit-(ConA/Gly)$_3$ConA/HRP film that lacks GOx: in this control, the film was tested by incubation in a solution containing H_2O_2 (0.01%) and $ABTS^{Red}$. As expected, this control film also became green upon incubation with H_2O_2. In contrast, the rightmost image shows that when such a GOx-free Chit-(ConA/Gly)$_3$ConA/HRP film was incubated with glucose and $ABTS^{Red}$, it remained colorless. These results demonstrate that both enzymes were successfully assembled into the multilayer assembly to confer dual enzymatic function.

Molecular and Electrical Cuing of Multilayer Disassembly

As illustrated in Scheme 1b, under neutral conditions, ConA is a tetrameric protein with four sugar-binding sites which enables it to cross-link glycogen chains and also couple glycosylated proteins to the multilayer film. Under acidic conditions, the ConA tetramer is dissociated into dimers and acidification (pH < 5.5) has been used to trigger disassembly of ConA-based multilayers.[47,74,75] Here, we demonstrate that this pH-triggered film disassembly can be cued by independent acidification mechanisms to either confer molecular specificity to disassembly or to enable electrical inputs to cue film disassembly.

Molecular cuing of disassembly can be achieved by incorporating an acid-generating enzyme into the multilayer, and GOx serves as a simple model enzyme. To demonstrate this concept, we assembled a Chit-$(ConA/Gly)_3$ConA/GOx onto a standard gold electrode and monitored the film's function electrochemically. The "input" plots in Figure 4a show that in this experiment, the electrode was biased to a constant anodic voltage (+0.7 V) to allow the detection of the H_2O_2 product, and the film was exposed to varying glucose "input" concentrations. Figure 4a shows that when the multilayer was exposed to increasing but low glucose concentrations (1−5 mM), the anodic "output" current was observed to progressively increase, consistent with the film performing a sensor function (i.e., glucose measurement). When the multilayer was exposed to a higher glucose concentration (25 mM), the current was observed to undergo a significant transient increase followed by a decrease to zero. (We should note that very high glucose concentrations of ~125 mM can disassemble these multilayers through competitive binding of glucose to the ConA sugar-binding sites.[37]) The response observed in Figure 4a is consistent with the disassembly of the multilayer and loss of localized H_2O_2 generation at the electrode surface. To further demonstrate this loss of function, the electrode was added to a fresh buffer solution and exposed to low levels of glucose (1−5 mM), yet Figure 4a shows that no appreciable current output was observed.

To provide evidence that acidification triggered the multilayer disassembly, we prepared a separate Chit-$(ConA/Gly)_3$ConA/GOx film. This film was fabricated by first electrodepositing chitosan, peeling the chitosan from the electrode, and sequentially contacting it with the various solutions. This "free-standing" Chit-$(ConA/Gly)_3$ConA/GOx film was placed in phosphate-buffered (10 mM, pH 7.4) glucose solutions with the metacresol purple sodium salt pH indicator dye. As illustrated in Figure 4b, this pH indicator shows purple under neutral conditions and yellow under acidic conditions. When a low concentration of glucose (5 mM) was added to the solution and the film was incubated for 1 h, and the upper image in Figure 4b shows that the film remained intact and the buffer solution remained neutral. Subsequently, an aliquot of concentrated glucose solution was added to increase the glucose concentration to 25 mM. After incubating for 1 h, the lower image in Figure 4b shows the solution had been acidified and the film dissolved. This observation supports the conclusion that glucose cues multilayer disassembly through an acidification mechanism.

Electrical cuing of disassembly is enabled by the anodic electrolysis of water. To demonstrate this concept, a Chit-$(ConA/Gly)_3$ConA/GOx film was assembled onto a standard electrode. As shown by the schemes and "input" plots in Figure 5a, the electrode

was first biased to a low anodic voltage (+ 0.7 V) to detect GOx function (e.g., the glucose-dependent generation of H_2O_2). The “output” plot in Figure 5a shows that at this low initial voltage, the addition of glucose aliquots resulted in stepwise increases in oxidation currents consistent with GOx sensing function. Next, the input oxidative voltage was increased (+ 1.5 V) to initiate a H^+-generating electrolysis reaction (i.e., to trigger disassembly). The output plot shows that at this high voltage, a sharp 200-fold increase in oxidation current is drawn consistent with water electrolysis. Finally, the electrode was transferred to a fresh buffer solution; the input plots show that a lower oxidative input voltage was imposed (+ 0.7 V) and aliquots of glucose were added (1−5 mM). No appreciable output currents were observed under these conditions indicating that the multilayer had disassembled in response to the high imposed oxidative voltage.

Independent evidence for electrically cued multilayer disassembly was provided in Figure 5b. To better visualize the film, the Pt electrode assembled with Chit-(ConA/Gly)$_3$ConA/GOx/HRP was incubated in ABTS (5 mM) and glucose (5 mM) solution for 4 h, and the film turned dark green (upper image in Figure 5b) because of the dual-enzyme reactions illustrated in Figure 5b. Next, the electrode was biased to an anodic voltage of +1.5 V for 10 min. As shown by the lower image in Figure 5b, the film dissolved as indicated by the color loss on the electrode. This result further supports the conclusion that the assembled multilayer can be disassembled in response to the electrical inputs.

CONCLUSIONS

In this work, we coupled electrodeposition and biospecific self-assembly mechanisms to create a biofunctional multilayer film. Electrodeposition of the pH-responsive self-assembling aminopolysaccharide chitosan provides the advantages of spatiotemporal and quantitative control of film fabrication. The ConA lectin can undergo biospecific and multivalent interactions which enable the layer-by-layer assembly of a glycogen-ConA multilayer and further allows protein-coupling to confer biofunctionality (e.g., for biosensing) through binding of a protein’s sugar moieties. One significant advantage of this biobased film fabrication approach is that by enlisting the intrinsic self-assembling capabilities of these biopolymers, film fabrication can be achieved simply and without the need for reactive reagents or complex instrumentation. This assembly approach may also be generic since various biological polymers can be electrodeposited[76,77] and diverse LbL mechanisms exist for multilayer assembly.[55,78,79] For instance, the electrodeposition of alginate[77] may enable extension to methods that require the initial film to be negatively charged (vs chitosan’s positive charge), while alternative lectins may confer different specificities for binding proteins with different glycanpatterns. Thus, this biopolymer-based self-assembling approach provides a biologically compatible, environmentally friendly, and sustainable route for the fabrication of functional films.

The hierarchical assembly of these films through reversible, noncovalent interactions enables these films to be cued to disassemble by external stimuli. In particular, glycogen-ConA multilayers disassemble under low pH conditions. We show that this low pH stimuli can be generated using an enzymatic reaction (i.e., the enzymatic oxidation of glucose) which provides the opportunity to confer molecular specificity to film disassembly. Further, we

show that anodic electrolytic reactions can trigger disassembly which provides a mechanism for disassembly to be cued by device-convenient electrical inputs. Thus, the assembly of hierarchical structures through reversible noncovalent interactions provides the opportunity to create dynamically responsive materials that could be useful for a range of emerging applications.[80–82]

It is interesting to note an important difference between stable assemblies and dynamically responsive assemblies. In particular, dynamically responsive assemblies are designed to be unstable (or responsive) to a specific condition−in our case, to a low pH. One concern is that dynamically responsive materials will be susceptible to adventitious cues that could trigger responses. For instance, a sample with a very low pH or a high sugar concentration could trigger disassembly of our films. In fact, previous studies have shown that very high glucose levels (125 mM) or lower concentrations of methyl-α-D-mannopyranoside (5 mM) can compete for ConA binding and thus trigger ConA-glycogen disassembly. A second concern is that dynamically responsive assemblies will respond to local conditions that may vary considerably from conditions in the bulk. In our case, the enzyme- and electrode-induced acid were generated locally. While the images in Figures 4 and 5 demonstrate that the films in our study were completely disassembled (i.e., dissolved), such disassembly may be impeded under conditions of high buffering or significant mixing that may suppress a local decrease in pH. Thus, it may be necessary to tailor dynamically responsive assemblies (e.g., GOx levels) for specific applications.

ACKNOWLEDGMENTS

This work was financially sponsored by the United States National Institute for Innovation in Manufacturing Biopharmaceuticals (NIIMBL QSP 1.23), the National Science Foundation (DMREF-1435957; CBET-1805274; ECCS-1807604), and the National Institute of Health (R21EB024102) as well as the National Natural Science Foundation of China (51573047) and the 111 project (B14018).

REFERENCES

(1). Zhang S Molecular Self-Assembly. Encycl. Mater. Sci. Technol 2001, 5822–5828.

(2). Philp D; Stoddart JF Self-Assembly in Natural and Unnatural Systems. Angew. Chem., Int. Ed. Engl 1996, 35, 1154–1196.

(3). Luo X; Lewandowski AT; Yi H; Payne GF; Ghodssi R; Bentley WE; Rubloff GW Programmable Assembly of a Metabolic Pathway Enzyme in a Pre-Packaged Reusable BioMEMS Device. Lab Chip 2008, 8, 420–430. [PubMed: 18305860]

(4). Fernandes R; Roy V; Wu H-C; Bentley WE Engineered Biological Nanofactories Trigger Quorum Sensing Response in Targeted Bacteria. Nat. Nanotechnol 2010, 5 (3), 213–217. [PubMed: 20081846]

(5). Gordonov T; Kim E; Cheng Y; Ben-Yoav H; Ghodssi R; Rubloff G; Yin J-J; Payne GF; Bentley WE Electronic Modulation of Biochemical Signal Generation. Nat. Nanotechnol 2014, 9 (8), 605–610. [PubMed: 25064394]

(6). Cheng Y; Tsao CY; Wu HC; Luo X; Terrell JL; Betz J; Payne GF; Bentley WE; Rubloff GW Electroaddressing Functionalized Polysaccharides as Model Biofilms for Interrogating Cell Signaling. Adv. Funct. Mater 2012, 22 (3), 519–528.

(7). Palermo V; Samorì P Molecular Self-Assembly across Multiple Length Scales. Angew. Chem., Int. Ed 2007, 46, 4428–4432.

(8). Segalman RA Materials Science. Directing Self-Assembly toward Perfection. Science (Washington, DC, U. S.) 2008, 321, 919–920.

(9). Capito RM; Azevedo HS; Velichko YS; Mata A; Stupp SI Self-Assembly of Large and Small Molecules into Hierarchically Ordered Sacs and Membranes. Science (Washington, DC, U. S.) 2008, 319, 1812–1816.

(10). Stupp SI Self-Assembly and Biomaterials. Nano Lett. 2010, 10, 4783–4786. [PubMed: 21028843]

(11). Luo X; Wu H-C; Tsao C-Y; Cheng Y; Betz J; Payne GF; Rubloff GW; Bentley WE Biofabrication of Stratified Biofilm Mimics for Observation and Control of Bacterial Signaling. Biomaterials 2012, 33 (20), 5136–5143. [PubMed: 22507453]

(12). Yang X; Kim E; Liu Y; Shi XW; Rubloff GW; Ghodssi R; Bentley WE; Pancer Z; Payne GF In-Film Bioprocessing and Immunoanalysis with Electroaddressable Stimuli-Responsive Polysaccharides. Adv. Funct. Mater 2010, 20, 1645–1652.

(13). Zhang S Emerging Biological Materials through Molecular Self-Assembly. Biotechnol. Adv. 2002, 20, 321–339. [PubMed: 14550019]

(14). Liu K; Kang Y; Wang Z; Zhang X 25th Anniversary Article: Reversible and Adaptive Functional Supramolecular Materials:“Non-covalent Interaction” Matters. Adv. Mater2013, 25 (39), 5530–5548. [PubMed: 24038309]

(15). Yang H; Yuan B; Zhang X; Scherman OA Supramolecular Chemistry at Interfaces: Host−Guest Interactions for Fabricating Multifunctional Biointerfaces. Acc. Chem. Res 2014, 47 (7), 2106–2115. [PubMed: 24766328]

(16). Wiradharma N; Tong YW; Yang Y-Y Self-Assembled Oligopeptide Nanostructures for Co-Delivery of Drug and Gene with Synergistic Therapeutic Effect. Biomaterials 2009, 30 (17), 3100–3109. [PubMed: 19342093]

(17). Ding Y; Kang Y; Zhang X Enzyme-Responsive Polymer Assemblies Constructed through Covalent Synthesis and Supramolecular Strategy. Chem. Commun 2015, 51 (6), 996–1003.

(18). Kopeček J; Yang J Smart Self-Assembled Hybrid Hydrogel Biomaterials. Angew. Chem., Int. Ed 2012, 51 (30), 7396–7417.

(19). Peng X; Liu Y; Bentley WE; Payne GF Electrochemical Fabrication of Functional Gelatin-Based Bioelectronic Interface. Biomacromolecules 2016, 17 (2), 558–563. [PubMed: 26752426]

(20). Payne GF; Kim E; Cheng Y; Wu H-C; Ghodssi R; Rubloff GW; Raghavan SR; Culver JN; Bentley WE Accessing Biology’s Toolbox for the Mesoscale Biofabrication of Soft Matter. Soft Matter 2013, 9 (26), 6019.

(21). Liu Y; Wu H-CC; Bhokisham NN; Li J; Hong K-LL; Quan DN; Tsao CY; Bentley WE; Payne GF Biofabricating Functional Soft Matter Using Protein Engineering to Enable Enzymatic Assembly. Bioconjugate Chem 2018, 29 (6), 1809–1822.

(22). Morrow BH; Payne GF; Shen J PH-Responsive Self-Assembly of Polysaccharide through a Rugged Energy Landscape. J. Am. Chem. Soc 2015, 137 (40), 13024–13030. [PubMed: 26383701]

(23). Redepenning J; Venkataraman G; Chen J; Stafford N Electrochemical Preparation of Chitosan/Hydroxyapatite Composite Coatings on Titanium Substrates. J. Biomed. Mater. Res 2003, 66A (2), 411–416.

(24). Wu LQ; Yi H; Li S; Rubloff GW; Bentley WE; Ghodssi R; Payne GF Spatially Selective Deposition of a Reactive Polysaccharide Layer onto a Patterned Template. Langmuir 2003, 19 (19), 519–524.

(25). Takahashi S; Sato K; Anzai J Layer-by-Layer Construction of Protein Architectures through Avidin−Biotin and Lectin−Sugar Interactions for Biosensor Applications. Anal. Bioanal. Chem 2012, 402 (5), 1749–1758. [PubMed: 21866404]

(26). Zhang C; Qu X; Li J; Hong H; Li J; Ren J; Payne GF; Liu C Biofabricated Nanoparticle Coating for Liver-Cell Targeting. Adv. Healthcare Mater 2015, 4 (13), 1972–1981.

(27). Qiu R; Regnier FE Use of Multidimensional Lectin Affinity Chromatography in Differential Glycoproteomics. Anal. Chem 2005, 77 (9), 2802–2809. [PubMed: 15859596]

(28). Morris TA; Peterson AW; Tarlov MJ Selective Binding of RNase B Glycoforms by Polydopamine-Immobilized Concanavalin A. Anal. Chem 2009, 81 (13), 5413–5420. [PubMed: 19514701]

(29). Forzan M; Marsh M; Roy P Bluetongue Virus Entry into Cells. J. Virol 2007, 81 (9), 4819–4827. [PubMed: 17267479]

(30). Nam H-J; Gurda BL; McKenna R; Potter M; Byrne B; Salganik M; Muzyczka N; Agbandje-McKenna M Structural Studies of Adeno-Associated Virus Serotype 8 Capsid Transitions Associated with Endosomal Trafficking. J. Virol 2011, 85 (22), 11791–11799. [PubMed: 21900159]

(31). Odegard AL; Kwan MH; Walukiewicz HE; Banerjee M; Schneemann A; Johnson JE Low Endocytic PH and Capsid Protein Autocleavage Are Critical Components of Flock House Virus Cell Entry. J. Virol 2009, 83 (17), 8628–8637. [PubMed: 19553341]

(32). Tanaka H; Sato Y; Harashima H; Akita H Cellular Environment-Responsive Nanomaterials for Use in Gene and SiRNA Delivery: Molecular Design for Biomembrane Destabilization and Intracellular Collapse. Expert Opin. Drug Delivery 2016, 13 (7), 1015–1027.

(33). Du J-Z; Du X-J; Mao C-Q; Wang J Tailor-Made Dual PH-Sensitive Polymer−Doxorubicin Nanoparticles for Efficient Anticancer Drug Delivery. J. Am. Chem. Soc 2011, 133 (44), 17560–17563. [PubMed: 21985458]

(34). Thermo scientific. Optimize Elution Conditions for Immunoaffinity Purification. Meridian 2009.

(35). Senear DF; Teller DC Thermodynamics of Concanavalin A Dimer-Tetramer Self-Association: Sedimentation Equilibrium Studies. Biochemistry 1981, 20 (11), 3076–3083. [PubMed: 7248268]

(36). Brewer CF; Marcus DM; Grollman AP; Sternlicht H Interactions of Saccharides with Concanavalin A. Relation between Calcium Ions and the Binding of Saccharides to Concanavalin A. J. Biol. Chem 1974, 249, 4614–4616. [PubMed: 4367220]

(37). Li J; Qu X; Payne GF; Zhang C; Zhang Y; Li J; Ren J; Hong H; Liu C Biospecific Self-Assembly of a Nanoparticle Coating for Targeted and Stimuli-Responsive Drug Delivery. Adv. Funct. Mater 2015, 25 (9), 1404–1417.

(38). Ge J; Neofytou E; Cahill TJ; Beygui RE; Zare RN Drug Release from Electric-Field-Responsive Nanoparticles. ACS Nano 2012, 6 (1), 227–233. [PubMed: 22111891]

(39). Neumann SE; Chamberlayne CF; Zare RN Electrically Controlled Drug Release Using PH-Sensitive Polymer Films. Nanoscale 2018, 10 (21), 10087–10093. [PubMed: 29781009]

(40). Samanta D; Hosseini-Nassab N; Zare RN Electro-responsive Nanoparticles for Drug Delivery on Demand. Nanoscale 2016, 8 (17), 9310–9317. [PubMed: 27088543]

(41). Samanta D; Mehrotra R; Margulis K; Zare RN On-Demand Electrically Controlled Drug Release from Resorbable Nanocomposite Films. Nanoscale 2017, 9 (42), 16429–16436. [PubMed: 29058737]

(42). Wu LQ; Gadre AP; Yi H; Kastantin MJ; Rubloff GW; Bentley WE; Payne GF; Ghodssi R Voltage-Dependent Assembly of the Polysaccharide Chitosan onto an Electrode Surface. Langmuir 2002, 18 (22), 8620–8625.

(43). Wu S; Wang W; Yan K; Ding F; Shi X; Deng H; Du Y Electrochemical Writing on Edible Polysaccharide Films for Intelligent Food Packaging. Carbohydr. Polym. 2018, 186, 236–242. [PubMed: 29455983]

(44). Che A-F; Liu Z-M; Huang X-J; Wang Z-G; Xu Z-K Chitosan-Modified Poly(Acrylonitrile- Co -Acrylic Acid) Nanofibrous Membranes for the Immobilization of Concanavalin A. Biomacromolecules 2008, 9 (12), 3397–3403. [PubMed: 18950224]

(45). Sato K; Anzai J Fluorometric Determination of Sugars Using Fluorescein-Labeled Concanavalin A−Glycogen Conjugates. Anal. Bioanal. Chem 2006, 384 (6), 1297–1301. [PubMed: 16477422]

(46). Sato K; Imoto Y; Sugama J; Seki S; Inoue H; Odagiri T; Hoshi T; Anzai J Sugar-Induced Disintegration of Layer-by-Layer Assemblies Composed of Concanavalin A and Glycogen. Langmuir 2005, 21 (2), 797–799. [PubMed: 15641859]

(47). Zhu Y; Tong W; Gao C Molecular-Engineered Polymeric Microcapsules Assembled from Concanavalin A and Glycogen with Specific Responses to Carbohydrates. Soft Matter 2011, 7 (12), 5805–5815.

(48). Sato K; Kodama D; Endo Y; Anzai J-I Preparation of Insulin-Containing Microcapsules by a Layer-by-Layer Deposition of Concanavalin A and Glycogen. J. Nanosci. Nanotechnol 2009, 9 (1), 386–390. [PubMed: 19441323]

(49). Jan U; Khan AA; Husain Q A Study on the Comparative Stability of Insoluble Complexes of Glucose Oxidase Obtained with Concanavalin A and Specific Polyclonal Antibodies. World J. Microbiol. Biotechnol 2006, 22 (10), 1033–1039.

(50). Pallarola D; Queralto N; Azzaroni O Supramolecular Assembly of Glucose Oxidase on Concanavalin A — Modified Gold Electrodes. Phys. Chem. Chem. Phys 2010, 12 (28), 8071–8083. [PubMed: 20526515]

(51). Wang B; Anzai JI Recent Progress in Lectin-Based Biosensors. Materials 2015, 8 (12), 8590–8607. [PubMed: 28793731]

(52). Farooqi M; Saleemuddin M; Ulber R; Sosnitza P; Scheper T Bioaffinity Layering: A Novel Strategy for the Immobilization of Large Quantities of Glycoenzymes. J. Biotechnol 1997, 55 (3), 171–179. [PubMed: 9249993]

(53). Song Y; Shen Y; Chen J; Song Y; Gong C; Wang L A PH-Dependent Electrochemical Immunosensor Based on Integrated Macroporous Carbon Electrode for Assay of Carcinoembryonic Antigen. Electrochim. Acta 2016, 211, 297–304.

(54). Song Y; Liu H; Tan H; Xu F; Jia J; Zhang L; Li Z; Wang L PH-Switchable Electrochemical Sensing Platform Based on Chitosan-Reduced Graphene Oxide/Concanavalin A Layer for Assay of Glucose and Urea. Anal. Chem 2014, 86 (4), 1980–1987. [PubMed: 24502773]

(55). Wang Y; Liu Y; Cheng Y; Kim E; Rubloff GW; Bentley WE; Payne GF Coupling Electrodeposition with Layer-by-Layer Assembly to Address Proteins within Microfluidic Channels. Adv. Mater 2011, 23 (48), 5817–5821. [PubMed: 22102376]

(56). Vogt S; Su Q; Gutiérrez-Sánchez C; Nöll G Critical View on Electrochemical Impedance Spectroscopy Using the Ferri/Ferrocyanide Redox Couple at Gold Electrodes. Anal. Chem 2016, 88 (8), 4383–4390. [PubMed: 26990929]

(57). Patolsky F; Zayats M; Katz E; Willner I Precipitation of an Insoluble Product on Enzyme Monolayer Electrodes for Biosensor Applications: Characterization by Faradaic Impedance Spectroscopy, Cyclic Voltammetry, and Microgravimetric Quartz Crystal Microbalance Analyses. Anal. Chem 1999, 71 (15), 3171–3180. [PubMed: 10450161]

(58). Ben-Yoav H; Dykstra PH; Bentley WE; Ghodssi R A Controlled Microfluidic Electrochemical Lab-on-a-Chip for Label-Free Diffusion-Restricted DNA Hybridization Analysis. Biosens. Bioelectron 2015, 64, 579–585. [PubMed: 25310492]

(59). Kim K; Kwak J Faradaic Impedance Titration of Pure 3-Mercaptopropionic Acid and Ethanethiol Mixed Monolayers on Gold. J. Electroanal. Chem 2001, 512 (1−2), 83–91.

(60). Zhang Y; Thomas Y; Kim E; Payne GF PH- and Voltage-Responsive Chitosan Hydrogel through Covalent Cross-Linking with Catechol. J. Phys. Chem. B 2012, 116 (5), 1579–1585. [PubMed: 22229705]

(61). Hong S. a; Kwon J; Kim D; Yang S. A Rapid, Sensitive and Selective Electrochemical Biosensor with Concanavalin A for the Preemptive Detection of Norovirus. Biosens. Bioelectron 2015, 64, 338–344. [PubMed: 25254625]

(62). Alfonta L; Bardea A; Khersonsky O; Katz E; Willner I Chronopotentiometry and Faradaic Impedance Spectroscopy as Signal Transduction Methods for the Biocatalytic Precipitation of an Insoluble Product on Electrode Supports: Routes for Enzyme Sensors, Immunosensors and DNA Sensors. Biosens. Bioelectron 2001, 16 (9−12), 675–687. [PubMed: 11679244]

(63). Jin Z; Güven G; Bocharova V; Halámek J; Tokarev I; Minko S; Melman A; Mandler D; Katz E Electrochemically Controlled Drug-Mimicking Protein Release from Iron-Alginate Thin-Films Associated with an Electrode. ACS Appl. Mater. Interfaces 2012, 4 (1), 466–475. [PubMed: 22200073]

(64). Chang B-Y; Park S-M Electrochemical Impedance Spectroscopy. Annu. Rev. Anal. Chem 2010, 3 (1), 207–229.

(65). Yao H; Hu N PH-Switchable Bioelectrocatalysis of Hydrogen Peroxide on Layer-by-Layer Films Assembled by Concanavalin A and Horseradish Peroxidase with Electroactive Mediator in Solution. J. Phys. Chem. B 2010, 114 (9), 3380–3386. [PubMed: 20163095]

(66). Palazzo G; Colafemmina G; Guzzoni Iudice C; Mallardi A Three Immobilized Enzymes Acting in Series in Layer by Layer Assemblies: Exploiting the Trehalase-Glucose Oxidase-Horseradish

Peroxidase Cascade Reactions for the Optical Determination of Trehalose. Sens. Actuators, B 2014, 202, 217–233.

(67). Li F; Wang Z; Chen W; Zhang S A Simple Strategy for One-Step Construction of Bienzyme Biosensor by in-Situ Formation of Biocomposite Film through Electrodeposition. Biosens. Bioelectron. 2009, 24 (10), 3030–3035. [PubMed: 19395252]

(68). Zhang Y; Yong Y; Ge J; Liu Z Lectin Agglutinated Multienzyme Catalyst with Enhanced Substrate Affinity and Activity. ACS Catal. 2016, 6 (6), 3789–3795.

(69). Shan D; Cosnier S; Mousty C HRP Wiring by Redox Active Layered Double Hydroxides: Application to the Mediated H2O2detection. Anal. Lett 2003, 36 (5), 909–922.

(70). Nguyen LT; Yang KL Combined Cross-Linked Enzyme Aggregates of Horseradish Peroxidase and Glucose Oxidase for Catalyzing Cascade Chemical Reactions. Enzyme Microb. Technol 2017, 100, 52–59. [PubMed: 28284312]

(71). Lu S; Hu T; Wang S; Sun J; Yang X Ultra-Sensitive Colorimetric Assay System Based on the Hybridization Chain Reaction-Triggered Enzyme Cascade Amplification. ACS Appl. Mater. Interfaces 2017, 9 (1), 167–175. [PubMed: 27996245]

(72). Cao C; Kim E; Liu Y; Kang M; Li J; Yin JJ; Liu H; Qu X; Liu C; Bentley WE; Payne GP Radical Scavenging Activities of Biomimetic Catechol-Chitosan Films. Biomacromolecules 2018, 19 (8), 3502–3514. [PubMed: 29928797]

(73). Liu H; Qu X; Kim E; Lei M; Dai K; Tan X; Xu M; Li J; Liu Y; Shi X; Li P; Payne GP; Liu C Bio-Inspired Redox-Cycling Antimicrobial Film for Sustained Generation of Reactive Oxygen Species. Biomaterials 2018, 162, 109–122. [PubMed: 29438879]

(74). Yao H; Hu N PH-Switchable Bioelectrocatalysis of Hydrogen Peroxide on Layer-by-Layer Films Assembled by Concanavalin A and Horseradish Peroxidase with Electroactive Mediator in Solution. J. Phys. Chem. B 2010, 114 (9), 3380–3386. [PubMed: 20163095]

(75). Yao H; Gan Q; Peng J; Huang S; Zhu M; Shi K A Stimuli-Responsive Biosensor of Glucose on Layer-by-Layer Films Assembled through Specific Lectin-Glycoenzyme Recognition. Sensors 2016, 16 (4), 563.

(76). Peng X; Liu Y; Bentley WE; Payne GF Electrochemical Fabrication of Functional Gelatin-Based Bioelectronic Interface. Biomacromolecules 2016, 17 (2), 558–563. [PubMed: 26752426]

(77). Shi XW; Tsao CY; Yang X; Liu Y; Dykstra P; Rubloff GW; Ghodssi R; Bentley WE; Payne GF Electroaddressing of Cell Populations by Co-Deposition with Calcium Alginate Hydrogels. Adv. Funct. Mater 2009, 19 (13), 2074–2080.

(78). Manna U; Bharani S; Patil S Layer-by-Layer Self-Assembly of Modified Hyaluronic Acid/ Chitosan Based on Hydrogen Bonding. Biomacromolecules 2009, 10 (9), 2632–2639. [PubMed: 19694426]

(79). Wang B; Yoshida K; Sato K; Anzai J; Wang B; Yoshida K; Sato K; Anzai J Phenylboronic Acid-Functionalized Layer-by-Layer Assemblies for Biomedical Applications. Polymers (Basel, Switz.) 2017, 9 (12), 202.

(80). Wan P; Wang Y; Jiang Y; Xu H; Zhang X Fabrication of Reactivated Biointerface for Dual-Controlled Reversible Immobilization of Cytochrome C. Adv. Mater 2009, 21 (43), 4362–4365. [PubMed: 26042945]

(81). Liu X; Wang S Three-Dimensional Nano-Biointerface as a New Platform for Guiding Cell Fate. Chem. Soc. Rev 2014, 43 (8), 2385–2401. [PubMed: 24504119]

(82). Parlak O; Ashaduzzaman M; Kollipara SB; Tiwari A; Turner AP F. Switchable Bioelectrocatalysis Controlled by Dual Stimuli-Responsive Polymeric Interface. ACS Appl. Mater. Interfaces 2015, 7 (43), 23837–23847. [PubMed: 26440202]

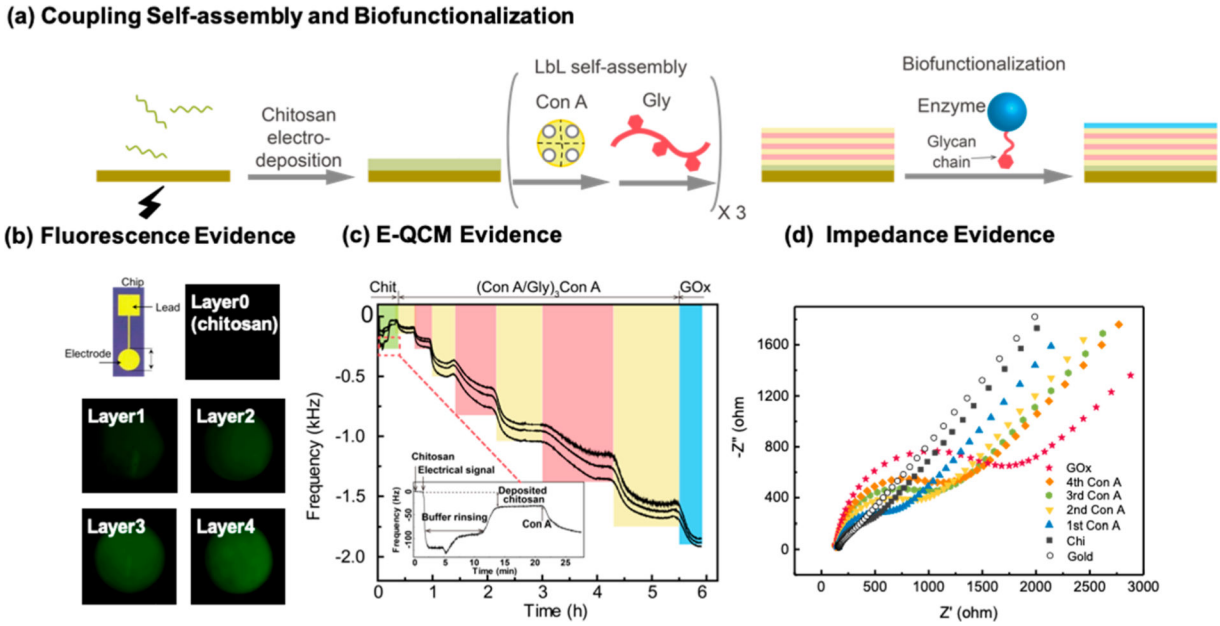

Figure 1.

Physical evidence for coupling of electro-induced self-assembly and LbL self-assembly. (a) Schematic illustrating the experimental procedures. (b) Fluorescence images of film fabricated with FITC-ConA indicate that electrodeposited chitosan serves as a template to enable spatially controllable LbL self-assembly. (c) E-QCM measurements demonstrate the electrodeposition of chitosan (inset) and LbL self-assembly of ConA, glycogen, and GOx. (d) The Nyquist plot indicates increasing impedance with the assembly of each additional glycogen-ConA layer and the final GOx layer.

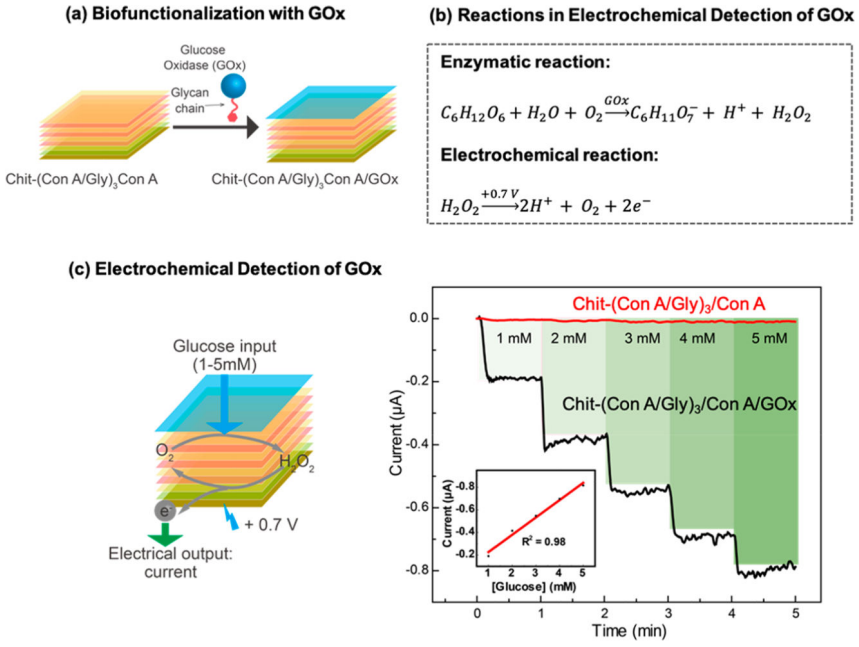

Figure 2.

Characterization of GOx biofunction. (a) Scheme illustrating the assembly of GOx to film through the binding between ConA and GOx glycan chains. (b) Electrochemical detection of GOx via GOx-catalyzed glucose oxidation and the subsequent electrochemical oxidation of H_2O_2 product.(c) Scheme and plots showing quantitative response in current output for glucose input with varying concentration and the inset showing corresponding standard curve.

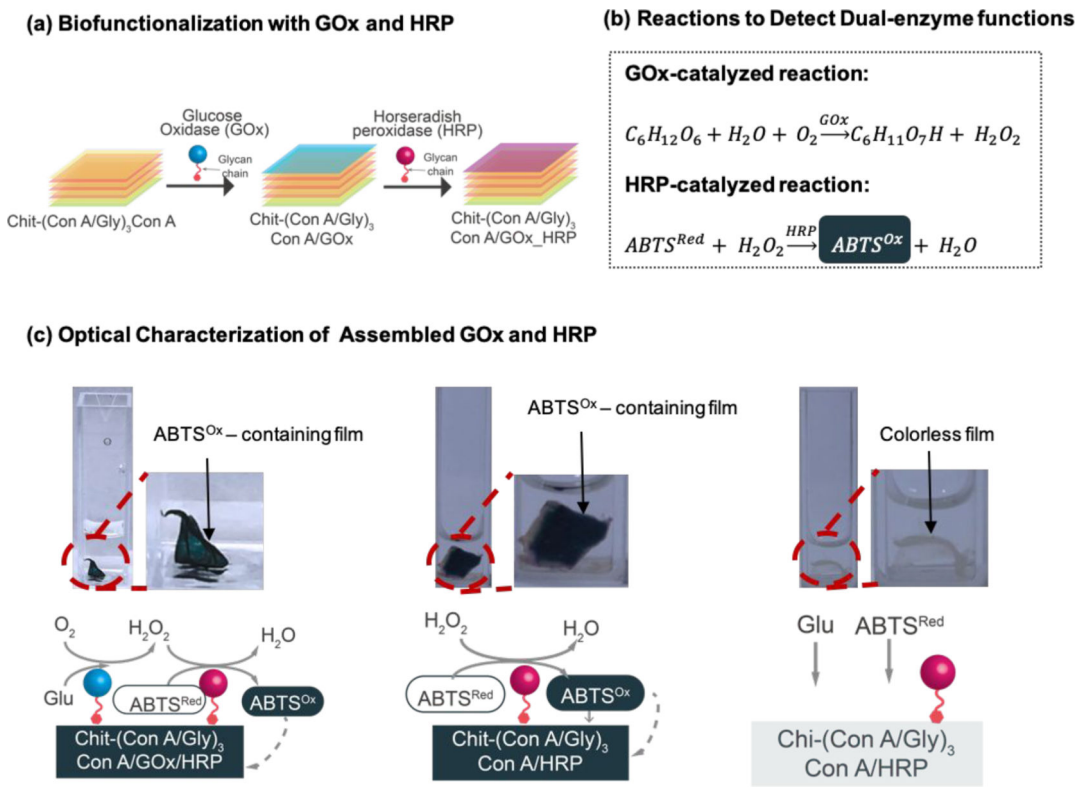

Figure 3.

Characterization of GOx and HRP biofunction. (a) Scheme illustrating the sequential assembly of GOx and HRP to film. (b) Detection of dual-enzyme functions via the GOx-catalyzed glucose oxidation and the subsequent HRP-catalyzed generation of dark green $ABTS^{Ox}$. (c) When film containing both GOx and HRP was treated with glucose and $ABTS^{Red}$, the film was observed to be dark green due to generation of $ABTS^{Ox}$ (left); the same color was observed for film containing only HRP with the treatment of H_2O_2 and $ABTS^{Red}$ (middle). However, in the absence of H_2O_2, the film was colorless (right).

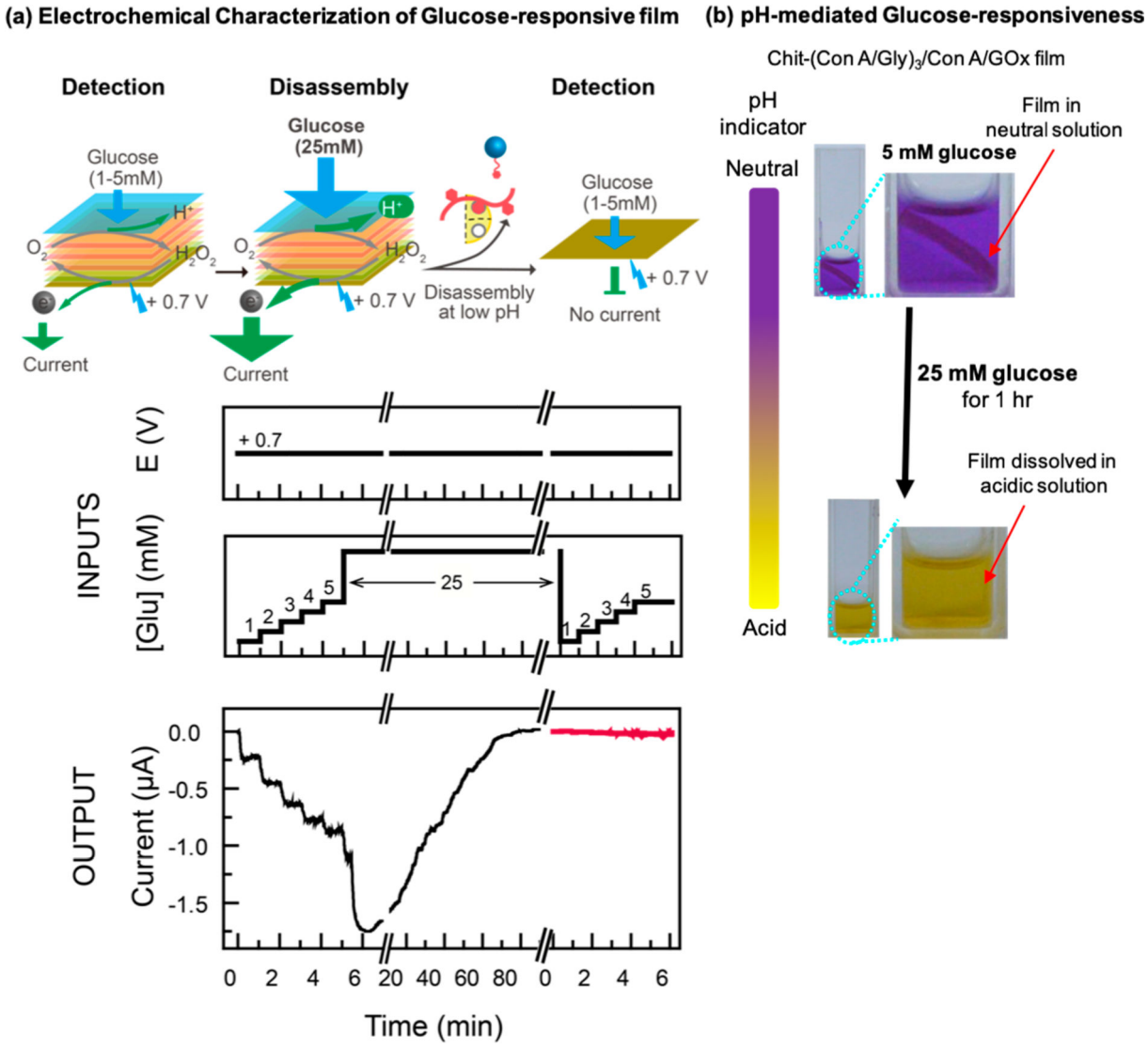

Figure 4.

Molecular Cuing of Disassembly. (a) The film-coated electrode was biased to a constant anodic voltage (+ 0.7 V) and first exposed to low levels of glucose (1−5 mM) to detect GOx activity and then exposed to high levels of glucose (25 mM) to cue the disassembly. No significant current output was observed when the film was exposed to low-level glucose again, indicating disassembly of film in response to high-level glucose. (b) The color change of the pH indicator dye and dissolution of the film under high-level glucose concentrations indicates that acidification is responsible for film disassembly.

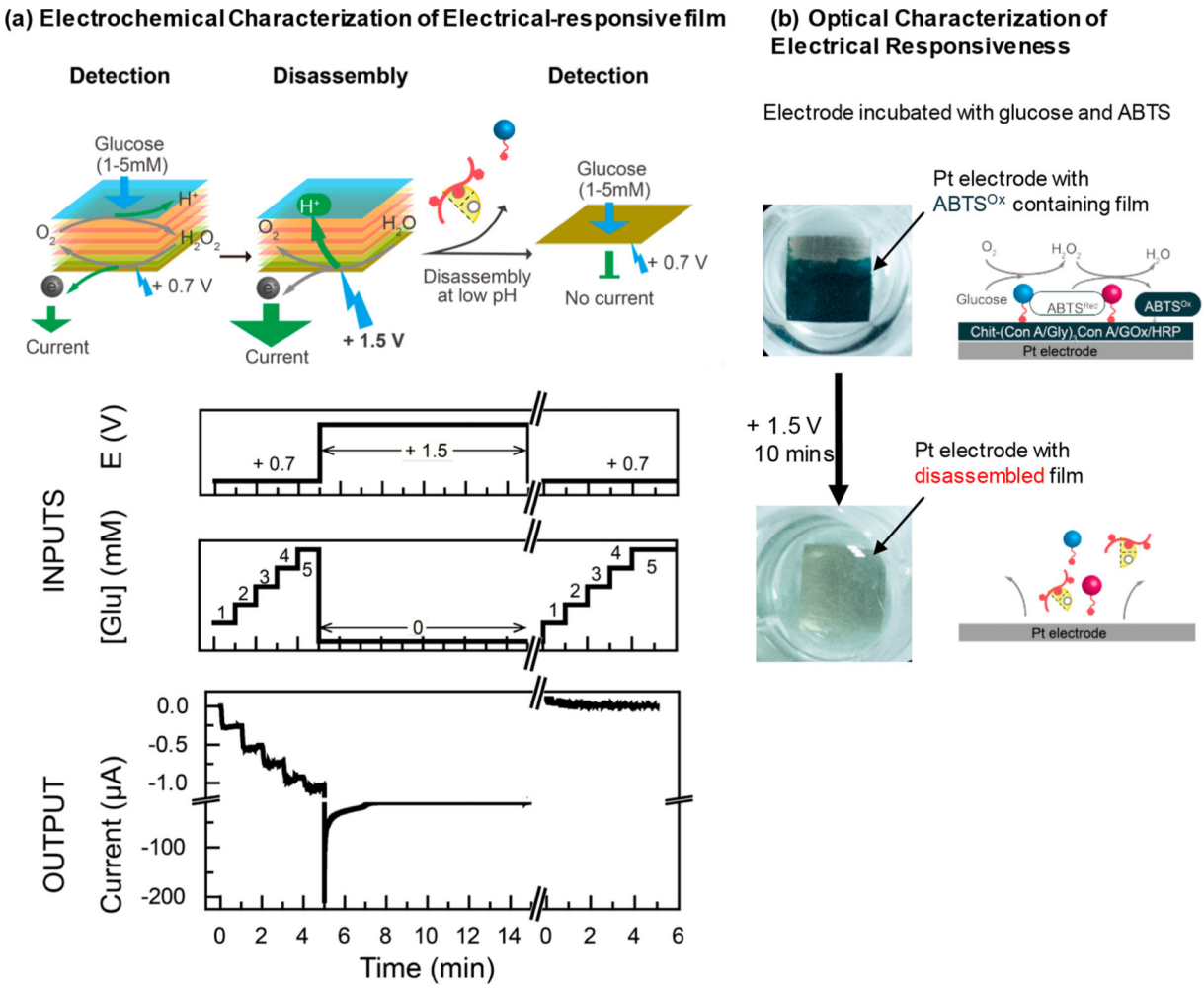

Figure 5.

Electrical Cuing of Disassembly. (a) The GOx sensing function was first evaluated electrochemically using a low oxidative voltage (+0.7 V), and then disassembly was cued using a higher oxidative voltage (+ 1.5 V). Afterward, the GOx function was tested again and no appreciable current out was observed, indicating disassembly of film. (b) Film containing GOx and HRP was observed to be dark green in the presence of glucose and $ABTS^{Red}$. The color was lost after the application of an oxidative voltage (+ 1.5 V) indicating that film disassembly was cued by the electrical signal.

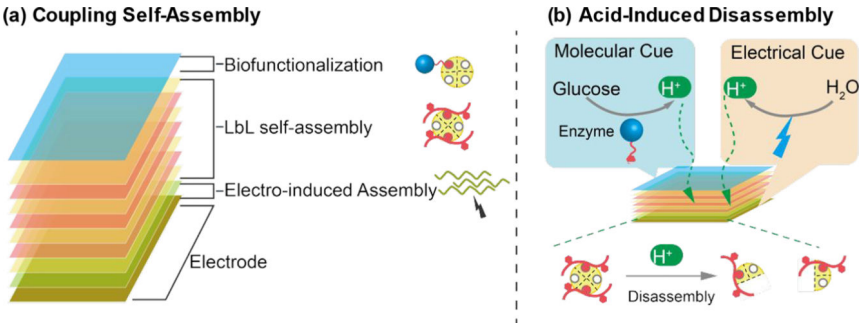

Scheme 1.

(a) Multilayer Film Fabricated by Coupling Two Self-Assembly Mechanisms: Electrodeposition of Chitosan and LbL Self-Assembly of ConA, Glycogen, and Glycoproteins; (b) Glucose and Electrical Signals Transduced into pH Changes to Cue the Disassembly of Films